Nat Hazards
DOI 10.1007/s11069-008-9273-z

ORIGINAL PAPER

Satellite detection of hazardous volcanic clouds and the risk to global air traffic

A. J. Prata

Received: 9 February 2008 / Accepted: 13 June 2008

Abstract Remote sensing instruments have been used to identify, track and in some cases quantify atmospheric constituents from space-borne platforms for nearly 30 years. These data have proven to be extremely useful for detecting hazardous ash and gas (principally SO_2) clouds emitted by volcanoes and which have the potential to intersect global air routes. The remoteness of volcanoes, the sporadic timings of eruptions and the ability of the upper atmosphere winds to quickly spread ash and gas, make satellite remote sensing a key tool for developing hazard warning systems. It is easily recognized how powerful these tools are for hazard detection and yet there has not been a single instrument designed specifically for this use. Instead, researchers have had to make use of instruments and data designed for other purposes. In this article the satellite instruments, algorithms and techniques used for ash and gas detection are described from a historical perspective with a view to elucidating their value and shortcomings. Volcanic clouds residing in the mid- to upper-troposphere (heights above 5 km) have the greatest potential of intersecting air routes and can be dispersed over many 1,000s of kilometres by the prevailing winds. Global air traffic vulnerability to the threat posed by volcanic clouds is then considered from the perspectives of satellite remote sensing, the upper troposphere mean wind circulation, and current and forecast air traffic density based on an up-to-date aircraft emissions inventory. It is concluded that aviation in the Asia Pacific region will be increasingly vulnerable to volcanic cloud encounters because of the large number of active volcanoes in the region and the increasing growth rate of air traffic in that region. It is also noted that should high-speed civil transport (HSCT) aircraft become operational, there will be an increased risk to volcanic debris that is far from its source location. This vulnerability is highlighted using air traffic density maps based on NOx emissions and satellite SO_2 observations of the spread of volcanic clouds.

Keywords Hazardous volcanic clouds · Global air traffic risk · Satellite measurements

A. J. Prata (✉)
Norwegian Institute for Air Research, P.O. Box 100, 2027 Kjeller, Norway
e-mail: fpr@nilu.no

1 Introduction

The unpredictability of volcanic eruptions (both in timing and in location) have led to many disasters. In modern historical times, catastrophes due to volcanic eruptions can be found in the literature, in some cases causing social, economic and political upheaval. Until the last 60 years or so, major hazards due to volcanic eruptions have been localized within the region surrounding the eruption. The most far-reaching effects have come from large eruptions which can disrupt the Earth's climate system on the time-scale of years. With the advent of inter-continental passenger jet travel, a new hazard from volcanic eruptions has emerged. Volcanic eruptions can inject large quantities of volcanic ash and gases into the atmosphere at heights that range from the summit of the volcano to as high as 50 km in the most energetic eruptions (e.g. Pinatubo, Philippines, 15.13° N, 20.35° E, 10–15 June, 1991). Once aloft, winds can transport the ash and gases rapidly and in multiple directions which depend on the wind speed and wind shear (the change in wind direction with height). Within the jet stream, wind speeds may reach 100 m s^{-1} (360 km hr^{-1}) so that transport over long distances in just a few hours is possible. The ash can cause extensive damage to aircraft, stalling engines, abrading windscreens and damaging sensitive avionics equipment (Casadevall 1994; Casadevall et al. 1996). Volcanic gases, specifically SO_2 may also pose a hazard to aircraft, and because gas and ash have different specific gravities they may separate and travel at different speeds and different heights in a sheared atmosphere (Holasek et al. 1996).

Coupled with the problem of forecasting the onset of eruptions and tracking their movement, is the difficulty of discriminating hazardous volcanic clouds from more common meteorological clouds. Even with the full knowledge of a volcanic eruption in progress, airline authorities do not have sufficient information to be able to confidently ensure the safety of jet aircraft. The logistical challenges faced by the airline industry are large: there are more than 70 volcanoes known to be active at present, eruptions occur on average about once per week somewhere over the globe, the eruptions are unpredictable, most volcanoes are remote and not routinely monitored, volcanic clouds can spread more than 1,000 km in less than 3 h and on board detection of these hazardous clouds is not currently possible (aircraft radar cannot detect micron size particles or gases). The current global airline fleet consists of about 18,000 aircraft and there is an increasing trend towards 2-engine jets, away from 4-engine aircraft. This is an important aspect in the assessment of aircraft safety as the ash directly affects the engines, causing them to stall. Having fewer engines exacerbates the risk of total loss of power and consequent disaster. Another development of concern is the proposed introduction of high-speed civil transport (HSCT) aircraft that will cruise at altitudes of 20 km or so. At these altitudes, as we shall see, there is greater likelihood of an encounter with volcanic debris far from its source. Forecasts suggest fleets of up to 1,000 HSCT aircraft may be operating by 2015 (Wei et al. 2001).

Satellite-based information provides a valuable asset to airline operations and this has been recognized for some time (Sawada 1987; Miller and Casadevall 1999). Initially, weather satellite data were used to monitor the movement of ash clouds, but later it was found that a combination of certain infrared channels could be used to discriminate ash clouds from meteorological clouds (Prata 1989a, b). Since these early discoveries and with satellite instrument technology advances, new and improved systems have been developed for ash detection and monitoring. These systems have also been applied to detect volcanic SO_2 gas. In this article we provide an overview of the advances made in utilizing satellite-based techniques for volcanic ash and gas detection and monitoring.

The article is organized as follows: we begin with a brief historical overview, reaching back 30 years to the start of the meteorological satellite era and describing how satellite instruments have been used to monitor and detect hazardous volcanic clouds. Next, the main techniques and progress made with satellite ash detection is presented, followed by a similar discussion for SO_2 detection. A threat analysis, based on the mean wind circulation and a proxy for air traffic density is developed to look at global and regional aviation vulnerabilities to hazardous volcanic clouds. Finally, some conclusions are made regarding the way that satellite data can be used to assist the aviation industry avoid hazardous volcanic clouds.

2 Historical overview

Sawada (1987) was the first person to provide a methodological survey of volcanic ash clouds and plumes using satellite imagery. He made use of geosynchronous weather satellite imagery (the Geostationary Meteorological Satellite—GMS[1]) to document volcanic eruptions and ash cloud dispersion within the western Pacific region. Sawada (1996) found that the detection rate from GMS imagery was about 13.7% of all known eruptions during the period late 1977–1985. This apparent low detection rate is attributed to the interference from meteorological clouds. Restrictions on the spatial (clouds smaller than about 5 km were not detectable) and spectral sampling (only single visible and infrared channels were available from GMS) also contributed to the low detection rate. Malingreau and Kaswanda (1986) used satellite imagery (AVHRR) to study the Colo, Indonesia eruption of 28 July, 1983, which is also known to have caused problems for jet aircraft operating in the region. Hanstrum and Watson (1983) studied the April, 1992 Galunggung, Indonesia eruptions from a meteorological perspective and noted the usefulness of satellite data in detecting ash plumes. Krueger (1983), Krueger et al. (1995) and Krueger et al. (2000) have shown that ultra-violet measurements from TOMS, designed to measure ozone, could be used to track volcanic SO_2 clouds. Carn et al. (2004) has shown that TOMS could also be used to measure man-made SO_2 emissions.

The theoretical basis for using infrared satellite imagery to discriminate volcanic ash clouds from meteorological clouds was provided in articles by Prata (1989a, b), and later extended by Wen and Rose (1994). The original method proposed by Prata (1989a) or variants of it are in use today by the Volcanic Ash Advisory Centres (VAACs). The method relies on taking the difference between two images acquired at two slightly different wavelengths within the infrared window, between 8 and 12 μm. Ash clouds are composed mostly of silicate particles and these absorb, scatter and re-emit infrared radiation in a different manner to ice and water, the main components of meteorological 'weather' clouds. This important difference allows a discrimination between clouds composed mostly of ash and those composed mostly of water and ice. When mixtures occur, as they invariably do in the turbulent atmosphere, the ability to discriminate is proportionally reduced, or in some instances rendered ineffective, for example when the ash particles are completely coated by ice (Rose et al. 1995). Despite some shortcomings of this "reverse absorption" technique, it remains the most effective means of detecting and discriminating volcanic ash clouds from satellite imagery.

In tandem with the developments of infrared satellite techniques, researchers had found that the ultra-violet portion of the electromagnetic spectrum could also be applied to the

[1] See the Appendix for a full list of all acronyms used in this article.

study of volcanic clouds. Krueger (1983) was the first to recognize the usefulness of satellite UV measurements for studying the spread of SO_2 in the eruption clouds from El Chichon, Mexico in 1982. He used TOMS UV imagery to show the movement of the SO_2 clouds around the globe. Originally designed to measure ozone, TOMS has now been providing detections of global volcanic SO_2 clouds for almost 30 years.

The principles behind using UV to measure and quantify volcanic substances (both SO_2 and volcanic ash can be identified) are described by Krueger et al. (1995) for the TOMS instrument and more recently by Krotkov et al. (2006) for the Ozone Monitoring Instrument (OMI). The SO_2 retrievals rely on the use of backscattered solar ultra-violet radiation that is preferentially affected by bands of SO_2 in the 280–320 nm wavelength range. The use of multiple bands permits separation of some of the confounding effects due to other molecules (e.g. O_3), reflections off the surface, Rayleigh multiple scattering and absorption by aerosols and clouds. Volcanic ash is detected by calculating an aerosol absorbing index (e.g. Torres et al. 1998) based on a ratio of two bands. Although this technique does not discriminate ash from other absorbing aerosols, the context of the measurements is usually sufficient to infer that ash is the aerosol responsible for the absorption.

Visible light has also been used to infer the presences of volcanic debris in the atmosphere. Matson (1984) used GOES and NOAA AVHRR satellite data and Richardson (1984) used NOAA AVHRR satellite data to measure the change in transparency of the atmosphere due to the eruption clouds of El Chichon.

These early attempts at utilizing satellite imagery in studying volcanic clouds were refined and improved after the major eruptions of Pinatubo, Philippines in June 1991. More than 30 cases of ash/aircraft encounters have been documented (Casadevall et al. 1996) and the mainly logistical problem of providing timely warnings to aircraft became apparent. Following the problems from this eruption, a network of ash advisory centres (VAACs) was set up, with nodes at Darwin, Australia, Tokyo, Japan, Anchorage, Alaska, Buenos Aires, Argentina, Montreal, Canada, Toulouse, France, Washington DC, USA and London, England. The VAACs provide advisories for their regions of responsibility and these cover the majority of the globe and include all the major air-routes. The operations of the VAACs are improving all the time—with the advent of satellite instruments with better spatial, temporal and spectral resolutions, and greatly improved data delivery services, much of the focus has moved from a reactive mode to a forecasting and pre-emptive mode. The forecasting of dispersing ash clouds has become a major activity of research and is discussed elsewhere in *this issue*. Logistical problems and operations at VAACs and at airports are also of major importance and are discussed by Guffanti and Albersheim (2008). Here we focus on satellite detection of volcanic clouds.

3 Volcanic ash detection from satellites

The problem of detecting volcanic clouds from satellites is really a problem of discrimination. Clouds absorb, emit and scatter radiation in the visible, infrared and microwave regions of the electromagnetic spectrum. At visible wavelengths, depending on the geometry of illumination (by the Sun or using a laser light source) and the geometry of observation, clouds may appear bright or dark. This is true of clouds of water, ice, silicates (volcanic ash), wind-blown dust (desert dust), smoke (e.g. from a large forest fire) or any other naturally or anthropogenically generated cloud of particles. It is sometimes very clear that a particular cloud is meteorological in origin (for example, a cloud of water droplets or ice particles, or a mixed phase cloud), but often not so clear that it is not a meteorological cloud. Figure 1a–h shows some satellite images of clouds and aerosols in the atmosphere. These are daytime MODIS images that have been enhanced to provide a "true-colour" rendition of the scene. In all scenes there are meteorological clouds and clouds due to other

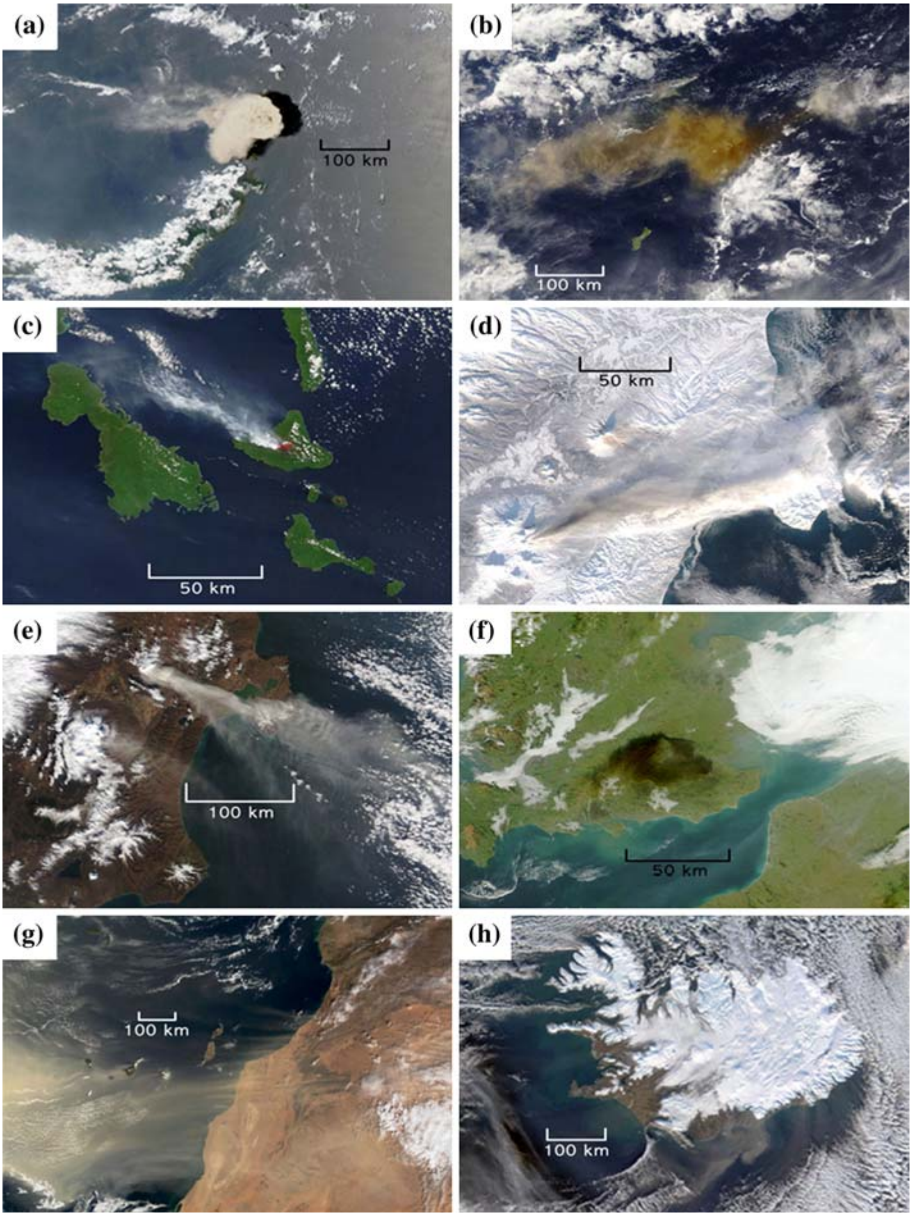

Fig. 1 Daytime MODIS scenes showing "anomalous" clouds. (**a**) Thick ash column from Ruang volcano, (**b**) drifting ash and gas plumes from Karthala volcano, (**c**) low-level gas cloud plume, (**d**) ash and gas plume over snow-covered terrain (Kluichevskoi volcano), (**e**) ash and gas plume from Kluichevskoi during the summer, (**f**) a noxious gas cloud from an industrial fire in southern England, (**g**) a dust outbreak over the Canary islands and (**h**) wind-blown ash streaming off the southern coast of Iceland

sources: (a) a thick ash column rising above Ruang volcano (Sangihie islands, Indonesia, 125.37° E, 2.30° N), (b) a drifting ash and gas plume recently emitted from Karthala volcano, Comoros (11.75°S, 43.38° E), (c) a low-level gas (predominantly SO_2 and H_2O) from Ambrym volcano, Vanuatu (16.25°S, 168.12° E), (d) an ash and gas plume over snow-covered terrain from Kluchevskoi volcano, Kamchatka (56.057° N, 160.638° E), (e) an ash and gas plume from Kluchevskoi, but in the summer, (f) a noxious cloud generated from an industrial accident in southern England, (g) a dust outbreak travelling westwards over the Canary Islands (28.00° N, 15.58° W) and (h) wind-blown ash off the coast of Iceland. These examples illustrate some of the variability found in anomalous clouds when viewed by satellites during the day. Some clouds appear almost black (Fig. 1f) or dark grey (Fig. 1h), some are as white as water/ice clouds (Fig. 1c and d), whilst others take various sandy shades with brown and yellow hues (Fig. 1a, b, e and g). By using objective analysis of daytime visible imagery alone, it has been very difficult to unambiguously discriminate ash clouds from other clouds. During the nighttime, the task is made even more difficult. This is the main reason why infrared data has proven to be of great use. There are now several ash detection algorithms in use or proposed, based on IR and visible satellite data. Table 1 shows a summary of ash detection schemes (with original references), based mostly on using infrared channels.

The two channel, reverse absorption technique is very useful in cases where the ash is not too thick and not too dispersed and is used at the VAACs (Watkin 2003). Figure 2 shows an application of the technique for the eruption of Karthala (Fig. 1b). In this case, the ash hazard is depicted using shades of yellow to red, with red suggesting more dense ash and greater hazard. Note that the white coloured clouds seen in the true colour image (Fig. 1b) of this event are not detected as an ash hazard. But note too that the edges of several clouds are detected as a potential ash hazard, whereas it seems more likely that these are meteorological clouds. The problems and pitfalls of using the reverse absorption technique have been discussed in the research literature (e.g. Simpson et al. 2000; Prata et al. 2001) and are well known to experienced meteorological analysts. Context is a key element in determining whether a particular cloud is an ash hazard or not, and trained meteorologists tasked with identifying ash clouds will use multiple sources of information including satellite imagery, pilot reports, ground observer reports, wind trajectories and background information regarding regional volcanic activity and prior behaviour.

Table 1 Summary of ash detection algorithms and techniques used with satellite infrared (IR) and visible channel data

Name	Principle	Reference
RA	2-band IR (11 and 12 μm)	Prata (1989a, b)
Ratio	2-band IR (11 and 12 μm)	Holasek and Rose (1991)
4-band	IR + visible	Mosher (2000)
TVAP	3-band IR (3.9, 11 and 12 μm)	Ellrod et al. (2003)
PCI	Multi-band principal components	Hillger and Clark (2002a, b)
WVC	2-band IR + water vapour correction	Yu et al. (2002)
RAT	3-band IR (3.5, 11, 12 μm)	Pergola et al. (2004)
3-band	3-band (IR and visible)	Pavolonis et al. (2006)

RA = Reverse absorption; TVAP = Three band volcanic ash product; PCI = Principle components; RAT = Ratio method; WVC = Water vapor correction method

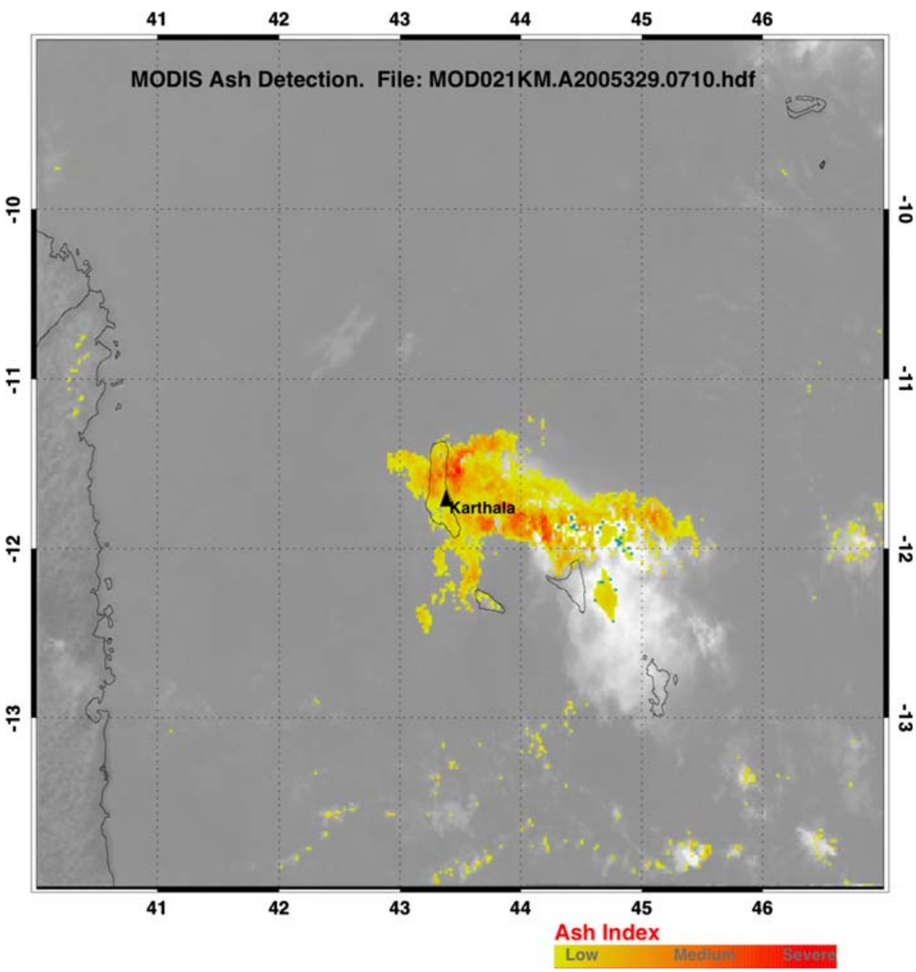

Fig. 2 An ash "risk" map for the Karthala eruption shown in Fig. 1b, based on the reverse absorption technique using two infrared channels. Regions of greatest risk are coloured red. Grey regions are believed to be "ash free"

It is possible to take the infrared analysis one step further. Wen and Rose (1994) and Prata and Grant (2001) have shown that by including a microphysical model of the ash particles with a detailed radiative transfer model, the infrared data can be inverted to reveal mean particle size and cloud opacity. When these parameters are integrated over the area covered by the cloud, the total mass and mass loading can be inferred from the data. These are quantifiable products that may be incorporated with dispersion models to generate risk maps for use by the aviation industry. An example of this kind of retrieval is given in Fig. 3, also for the Karthala eruption. There are many satellites (polar and geosynchronous) that carry these infrared channels, so this product can be delivered globally. Table 2 gives details of some of the satellite instruments capable of providing ash mass loadings.

Two of the instruments listed in Table 2 are capable of measuring much more than ash mass loadings. These instruments, AIRS (Chahine et al. 2006) and IASI (Clerbaux et al. 2007) have high spectral resolution and by utilizing more measurement channels it may be

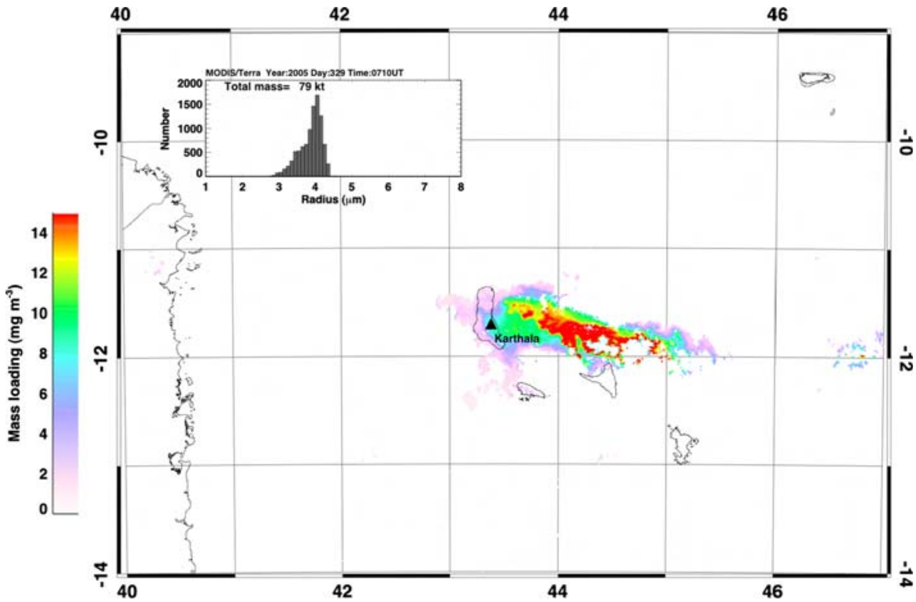

Fig. 3 Ash mass loading retrievals for the Karthala eruption shown in Fig. 1b

Table 2 Details of past and current satellite instruments that can be used to detect ash and generate ash mass loading maps from infrared measurements

Satellite	Instrument	Spatial resolution (km × km)	Temporal resolution (per day)	Time period covered (present)
NOAA	AVHRR-2, -3	1 × 1	2	1981
NOAA	HIRS-2, -3, -4	10 × 10[a]	2	1979
GOES	VISSR/VAS	5 × 5	24	1980
ENVISAT	ATSR-family	1 × 1	2[b]	1991
GMS-5	VISSR	5 × 5	24	1995
Terra/Aqua	MODIS	1 × 1	4[c]	1999
Aqua	AIRS	14 × 14	2	2002
MetOp	IASI	12 × 12	2	2007
MSG	SEVIRI	3 × 3	96	2006

[a] Earlier HIRS (1–3) instruments had a larger field of view of 18 × 18 km^2

[b] These satellite are in a 3-day repeat cycle, such that the same point imaged twice in one day will not be imaged again until 3 days later

[c] Assuming two satellites in orbit at any given time

possible to infer something about the mineralogy of the ash. Indeed it may also be possible to discriminate dust (Fig. 1g) and wind-blown ash (Fig. 1h) outbreaks from volcanic ash eruption clouds and plumes.

There remains some difficulty in identifying hazardous ash under many circumstances, and timeliness is still an issue. A further complication is that there is no standard satellite-based product providing ash cloud height. This vital piece of information is usually inferred later. Once a sequence of images has revealed the spatial and temporal behaviour of the ash cloud, trajectories are run based on "guessed" heights and the best fit is used to establish the most likely height of the hazardous ash cloud. This "hit and miss" methodology has recently been put on a firm theoretical basis by Eckhardt et al. (2008) who use an inverse modelling technique that combines Langrangian particle dispersion using wind fields with satellite measurements to estimate the injection height profile of the eruption. The method has been tested on the eruption of Jebel at Tair, Yemen (15.55° N, 41.83° E) and relied on SO_2 satellite measurements from SEVIRI as a proxy for ash. The result was very good and independent validation against OMI and a spaced-based lidar (CALIPSO) showed that once the injection height was known accurately (± 1 km) the trajectory and dispersion of the cloud could be faithfully tracked for several days and over more than 10,000 km. The idea of using SO_2 satellite measurements to infer the ash hazard is not new; but there are problems with this approach and ideally it would be better to use direct ash measurements. At the current time, satellite SO_2 measurements are easier to make and have proven to be very useful for aviation hazard warnings. The following section discusses the state of the science of SO_2 detection from space.

4 SO_2 detection from satellites

Sulphur dioxide is, typically, the third most abundant gas (after water vapour and CO_2) emitted by volcanoes. It is a colourless gas that can cause eye irritation, breathing difficulties and death when encountered in high concentrations. The background atmosphere contains very little SO_2—most anthropogenic emissions arise from industrial sources, whilst natural emissions are dominated by volcanic sources. Low-level SO_2 volcanic emissions (often referred to as passive degassing) are of little concern to aviation. During explosive eruption episodes, SO_2 may be violently injected into the atmosphere and may reach higher altitudes where they intercept the airways and potentially become a hazard to aviation. It is not clear exactly what threat SO_2 emissions pose to aircraft, however it is generally assumed that the emissions will be accompanied by ash, which is a known hazard. Consequently, pilots are trained to recognize the acrid odour generated by sulphur gases (SO_2 and H_2S both have characteristic pungent odours) so that they may infer that an encounter with a volcanic cloud has taken place. This may not mean that ash has been encountered—there are other tell-tale signs for an ash encounter—but the current procedures demand that if an encounter is suspected it should be noted, reported and any remedial maintenance checks carried out. It is possible that SO_2, in sufficiently high concentrations, could cause fuel contamination, and if encountered as sulphuric acid aerosol, it is believed that airframe and window damage could also occur (Bernard and Rose 1984). Under the assumption that volcanic SO_2 in the upper troposphere (above 5 km) travels with volcanic ash, it is sensible to use satellite measurements of SO_2 as a proxy for ash.

Since 1979, SO_2 has been measured by the TOMS instrument, designed to measure atmospheric ozone, on board several different polar-orbiting satellites. The measurements rely on scattered solar UV radiation, which is affected by the presence of SO_2 at wavelengths between 0.28 and 0.32 μm. The large footprint size (50×50 km^2), once per day coverage and relatively low signal-to-noise ratio for TOMS SO_2 measurements meant that only SO_2 clouds from the larger (VEI > 2) eruptions could be detected. Nevertheless, TOMS has proved to be very useful for tracking SO_2 clouds, and for verifying the volcanic origin of "anomalous" clouds. Good examples showing the collocation of SO_2 and ash clouds can be found in Schneider et al. (1999) and Constantine et al. (2000).

Table 3 Details of past and current satellite instruments that can be used to detect and quantify SO_2 using UV and IR measurements

Satellite	Instrument	Spatial resolution (km × km)	Temporal resolution (per day)	Time period covered (present)
Various	TOMS	50 × 50	1	1979
NOAA	HIRS-2, -3, -4	10 × 10[a]	2	1979
GOES	VISSR/VAS	5 × 5	24	1980
Terra/Aqua	MODIS	1 × 1	4[b]	1999
Terra	ASTER	0.09 × 0.09	1/16	1999
Aqua	AIRS	14 × 14	2	2002
Aura	OMI	24 × 13	1	2004
Aura	MLS	30 × 150	1	2004
ERS-2	GOME	320 × 40	1	1995
ENVISAT	SCIAMACHY	60 × 30	1	2002
MetOp	IASI	12 × 12	2	2007
MetOp	GOME-2	80 × 40	2	2007
MSG	SEVIRI	3 × 3	96	2006

[a] Earlier HIRS (1–3) instruments had a larger field of view of 18 × 18 km^2

[b] Assuming two satellites in orbit at any given time

The success of TOMS for detecting SO_2 using UV measurements has led to the development of improved instruments such as GOME, SCIAMACHY, OMI and GOME-2. The methods used for SO_2 detection are given by Eisinger and Burrows (1998) and Thomas et al. (2004) for GOME, by Richter et al. (2006) for SCIAMACHY and by Krotkov et al. (2006) for OMI. All of these instruments are in polar orbit and have, at best, spatial resolutions of 14 × 24 km^2 (OMI) and are restricted to coverage of the sunlit part of the Earth. GOME-2 and SCIAMACHY data are used to generate a global SO_2 alert for both natural (volcanic) and anthropogenic emissions (Van Geffen et al. (2007), see also http://www.oma.be/BIRA-IASB/Molecules/SO2nrt/) and a similar system is under construction for OMI.

SO_2 can also be measured using infrared radiation (Prata et al. 2003), with lower accuracy and precision than by using UV radiation. Polar-orbiting and geosynchronous satellite instruments exist with infrared channels that can be used to infer SO_2 column abundances. Satellite instruments starting in 1979 that can be used to measure SO_2 column amount include: HIRS, VISSR, MODIS, AIRS, SEVIRI and IASI.[2] Since all of these satellite data can be used during the night just as well as during the day, and because they generally have better spatial resolutions (up to 1 km^2), they also offer the possibility of developing a global SO_2 alert system. The main details regarding the UV and IR instruments for SO_2 detection are summarized in Table 3.

There have been many examples of the extensive spread of SO_2 from volcanic eruptions detected by both UV and IR satellite sensors. Notable amongst these are El Chichon (17.360° N, 92.228° W) in 1982 (Krueger 1983), Mt Spurr (61.299° N, 152.251° W) in 1989 (Schneider et al. 1995), Pinatubo in 1991 (Bluth et al. 1993; Prata et al. 2003) and Hudson (45.90° S, 72.97° W) in 1991 (Barton et al. 1992). More recently, OMI and AIRS

[2] ASTER can also be used to detect volcanic SO_2 (e.g. Urai 2004), but its long re-visit time (16 days) and narrow swath width (~60 km) make it less useful for global aviation threat monitoring.

measurements have tracked clouds of SO_2 generated by eruptions from Soufriere Hills, Montserat (16.72° N, 62.18° W) (Carn et al. 2007; Prata et al. 2007) and Jebel at Tair, Yemen (Eckhardt et al. 2008). These SO_2 clouds could be tracked for several weeks as they travelled with the prevailing winds at heights greater than 15 km. At these heights the SO_2 clouds were above commercial jet aircraft traffic and posed little threat to aviation, but this may not always be the case. The ability to track and forecast the movement of hazardous clouds using satellite-based SO_2 measurements is of great value and as indicated earlier, global alert systems have been developed to provide aviation warnings using these data.

5 The global threat to aviation from volcanic eruption clouds

Volcanic clouds move with the prevailing winds at the height of injection. At the onset of an eruption, it is likely that ash and gases are spread throughout the vertical column up to the maximum height reached by the cloud, which depends on the energetics of the eruption with some dependency on environmental conditions. During the first few hours of eruption, the vicinity in the neighbourhood of the volcano poses the greatest threat to aviation. Usually precursor information about the activity of the volcano is available and aviation is alerted well before an eruption occurs. Following a significant eruption, the ash and gases can be transported over great distances, but are usually confined to a much smaller vertical range of 1–2 km. Dispersion modelling of the movement of the cloud then depends critically on knowledge of the location of the cloud in the vertical, and less on the wind fields, as these are generally known more accurately. Current practice is to guess the height of the cloud based upon trial-and-error fits between observations of the clouds and model runs. VAACs use this information cautiously, together with other sources of information. They will advise that airspace is affected from the ground up to the suspected maximum height of the volcanic cloud, and express this in aviation terminology using flight levels, e.g. FL 350 means a pressure altitude of 35,000 ft or 10,700 m. Air traffic should then divert around a rather large spatial region which covers the horizontal location of the cloud and the vertical region from the ground up to FL X, where X is the designated flight level affected. While this strategy is risk averse, it can be a financial burden and perhaps unnecessary for the operator. This is because the volcanic cloud will, in most cases, be confined in the vertical to a layer of 1–2 km thickness and may not contain ash. The residence time of fine ash in the upper troposphere is of the order of several hours to a few days, and in a dispersed state the ash may not be a hazard to aircraft, although some case studies seem to indicate even undetected, very low concentration ash clouds may still pose a threat (Pieri et al. 2002; Tupper et al. 2004). Given the range of uncertainties present in predicting volcanic eruption activity, in knowledge of the injection height profile of an eruption and in establishing the minimum ash concentration level that is still dangerous to aviation, only fairly general indications of vulnerability can be established.

The mid- and upper-troposphere (MUT) wind circulation patterns are fundamental to establishing the hazard posed to commercial inter-continental aviation from dispersing volcanic clouds. In the MUT, zonal winds are stronger than meridional winds and consequently volcanic clouds tend to travel rapidly in the zonal direction. The long-term mean zonal wind fields at 250 hPa (10 km) are shown in Fig. 4 for the months of January (Fig. 4a) and July (Fig. 4b). Most notable in these plots are the strong zonal jets at roughly 30° N in January and 30° S in July. Zonal winds are generally quite weak ±10° latitude either side of the equator, but there is a noticeable seasonal dependence, with easterlies

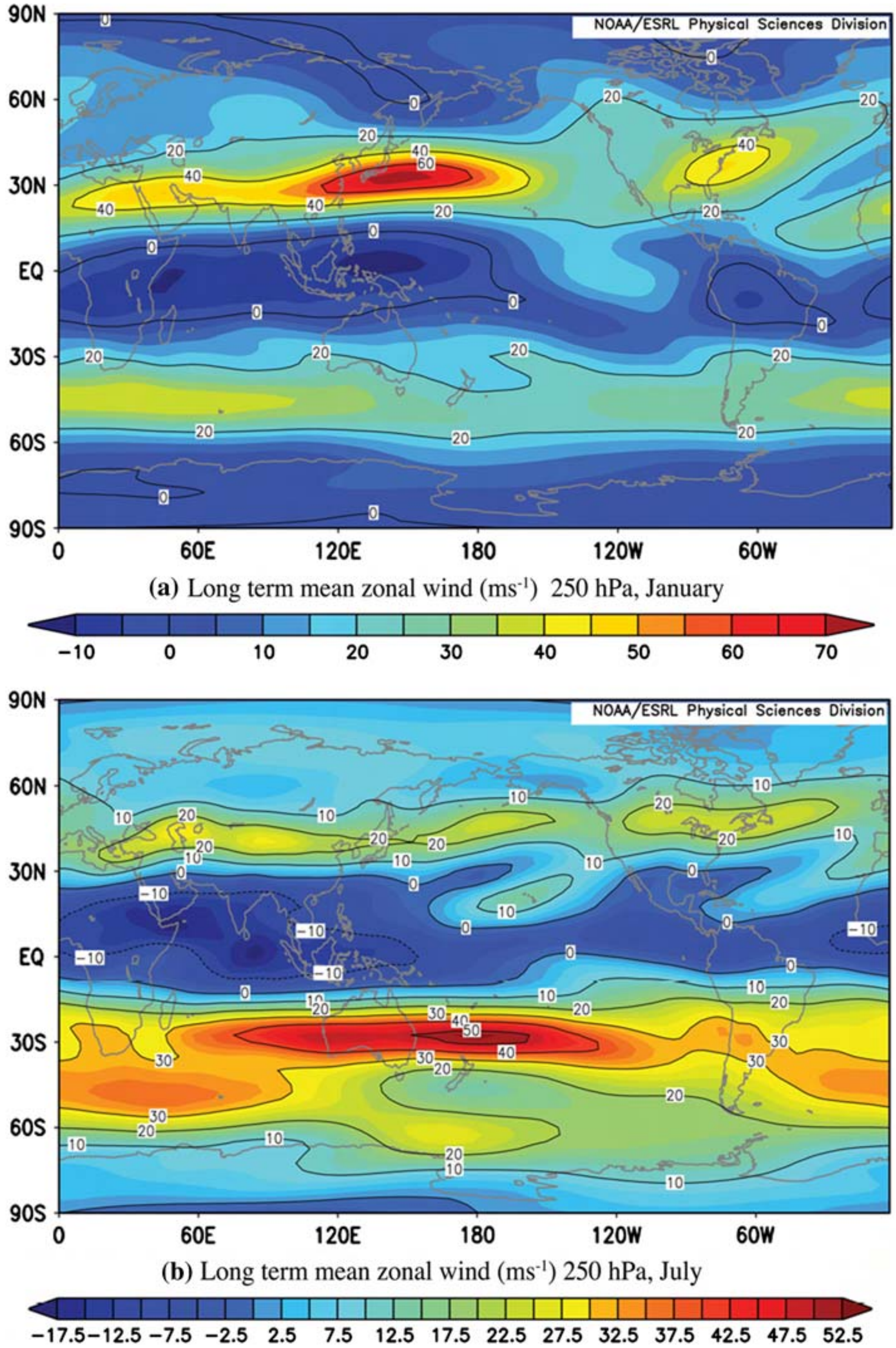

Fig. 4 Long-term mean zonal winds in m s^{-1} for (**a**) January and (**b**) July (Reproduced from NOAA/ESRL Physical Sciences Division, see: http://www.cdc.noaa.gov/cgi-bin/PublicData/getpage.pl)

dominating at latitudes north of the equator in July. Similar plots of the mean meridional wind component for January and July are shown in Fig. 5a, b. Meridional winds in January tend to be more northerly and can reach 6 m s^{-1} in the high latitudes of the winter hemisphere. Equatorial winds are weak at both times of the year. Some general comments can be made about the likely spread of volcanic clouds that reach 10 km altitude based on these mean wind circulation patterns. For eruptions that occur near equatorial latitudes in July, the dispersion will most likely be westwards with little transport polewards. In fact this was observed for the eruption of Pinatubo for clouds that reached much higher altitudes, since the wind structure at 10 km is similar up to 30 km or so (see Fig. 6). Eruptions that occur at higher latitudes will spread volcanic debris in directions and at speeds that depend on the hemisphere and the season. In July, Chilean eruption clouds will travel rapidly eastwards and southwards and it is very unlikely the clouds will spread to the northern hemisphere and more likely they will be confined to circumnavigate the southern hemisphere at latitudes south of 30° S. This was observed for the August, 1991 eruption of Mt Hudson, which spread volcanic clouds eastwards towards Australia causing some minor aviation incidents (Barton et al. 1992). Eruptions occurring in Japan and northwards along the Kamchatkan peninsula will spread clouds eastwards and at greater speeds in January than in July. The meridional winds will take these clouds southwards in summer (July) and northwards in winter (January). The north-eastward spreading of volcanic clouds emanating from Japanese or Kamchatkan volcanoes in winter is likely to create greater risk for aviation using the busy north Pacific air routes that connect Japan to the USA.

The main air corridor connecting air traffic between USA and continental Europe lies between latitudes 45–65° N and crosses the north Atlantic—the so-called North Atlantic Tracks (NATs). Volcanic eruptions from Iceland could potentially disrupt air traffic using the NATs. Greatest impact would occur when meridional winds are northerly and zonal winds weak. This would bring clouds southwards directly intersecting the NATs. A wintertime eruption fits this scenario better than a summertime event. At lower altitudes (<5 km) the meridional winds in January tend to be southerly, keeping lower altitude eruption clouds away from Europe and the main air routes. A more typical trajectory for volcanic clouds originating from Iceland is transport eastwards with northward confinement and circumnavigation of the pole. While this trajectory has been documented (Carn et al. 2008), it is a much less serious threat to aviation, due to the low density of air traffic at these high latitudes. Another possible trajectory for Icelandic eruption clouds consists of rapid eastward and then southward transport which brings the clouds over eastern Europe and into the busy continental air routes. This trajectory has also been documented from an eruption of Grimsvotn in 2004 (Witham et al. 2007), which caused some grounding of European aviation but no serious incidents were reported.

Over the busy (especially for air freight) trans-Pacific air routes between Japan and Asia and continental USA, the main threat is from Japanese volcanoes, volcanoes in Kamchatka and volcanoes along the Aleutian chain and into south-western Alaska. The whole region is volcanically active and there have been several aviation related incidents with ash clouds generated by volcanoes in this region. At most times of the year the zonal winds travel eastwards, taking volcanic debris from Japan/Kamchatka towards continental USA and into higher density air traffic. Two well-documented cases of aviation incidents have occurred in this region, both during the winter season. In the case of the KLM 747 commercial jet on route to Anchorage, Alaska from Amsterdam, Netherlands the encounter occurred in December 1989 and close to the Mt Redoubt volcano (60.485° N, 152.742° W) (Casadevall 1994). The aircraft was travelling south-eastwards towards the ash plume, which was moving north-westwards, with the mean winter winds (see Figs. 4a and 5a).

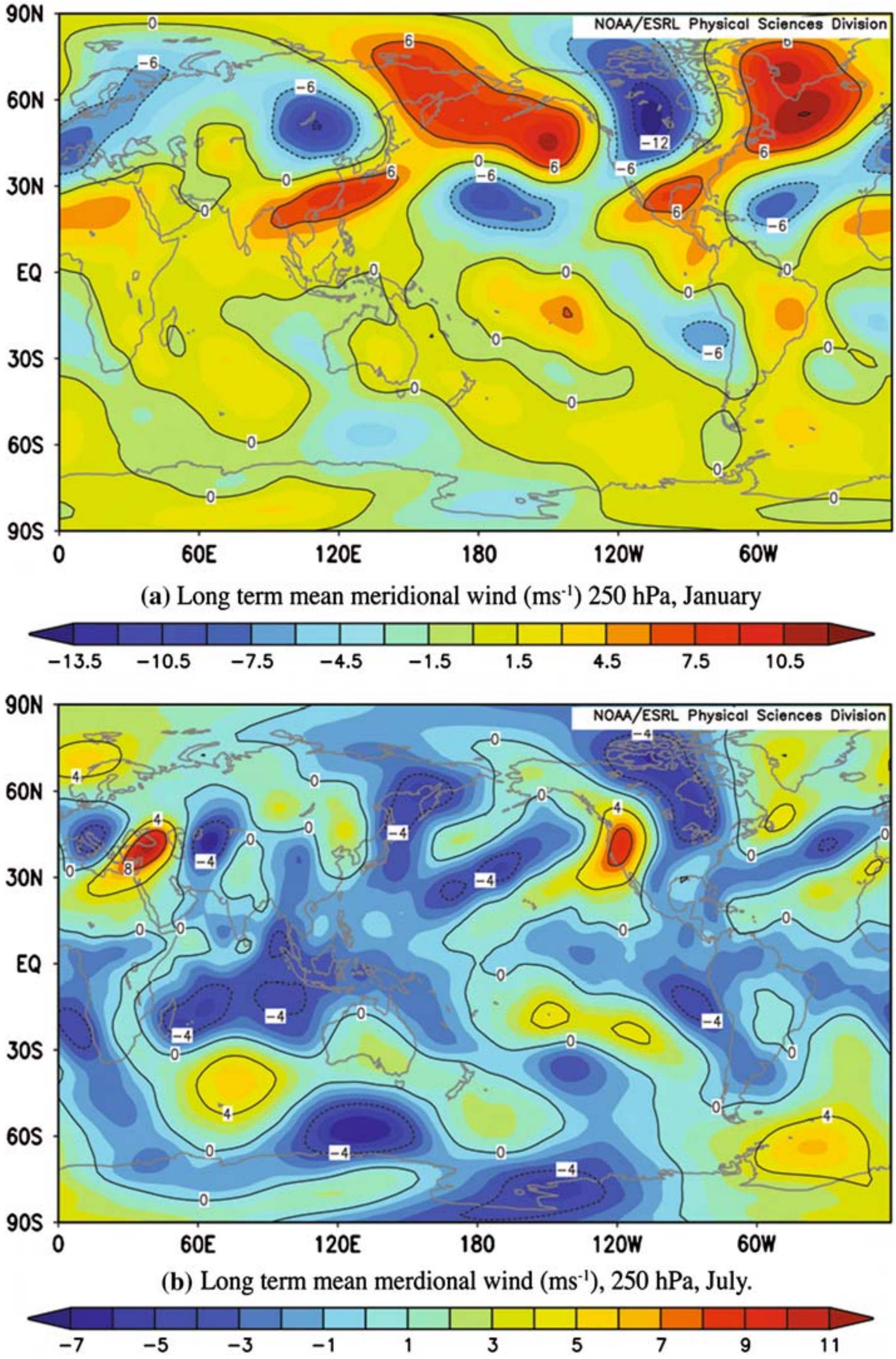

(**a**) Long term mean meridional wind (ms-1) 250 hPa, January

(**b**) Long term mean merdional wind (ms-1), 250 hPa, July.

Fig. 5 Long-term mean meridional winds in m s^{-1} for (**a**) January and (**b**) July (Reproduced from NOAA/ESRL Physical Sciences Division, see: http://www.cdc.noaa.gov/cgi-bin/PublicData/getpage.pl)

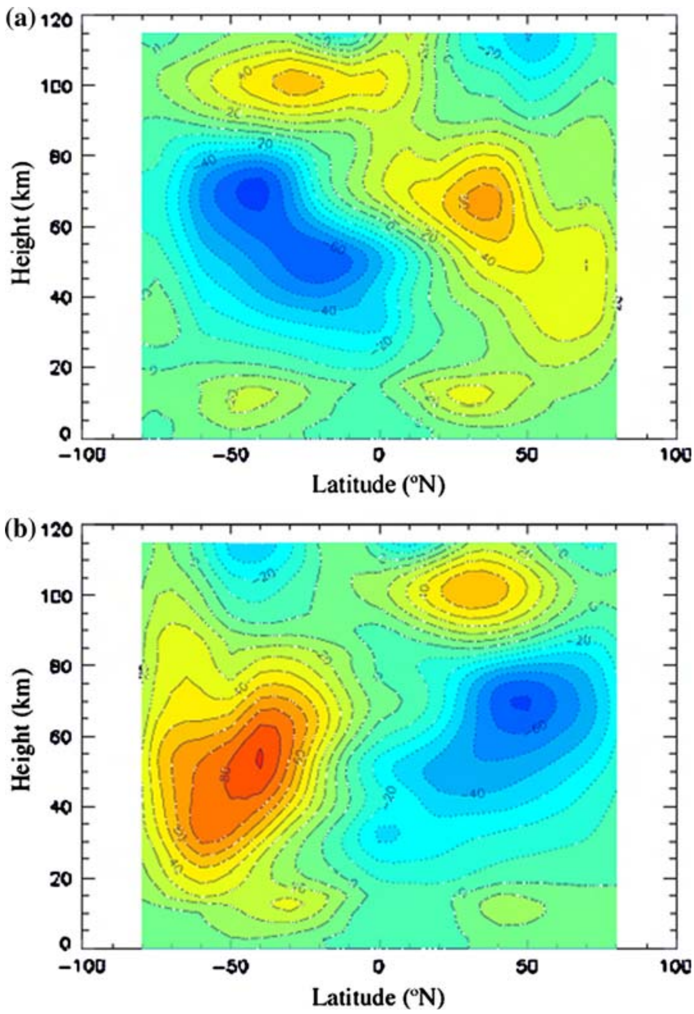

Fig. 6 Latitude-height cross-sections of the mean zonal winds for (**a**) January and (**b**) July (*After* Fleming et al. 1988)

A dispersion model (PUFF) animation of this encounter can be found at: http://puff.images.alaska.edu/Redoubt_webpage/Puff_redoubt_ash.shtml. A more recent event in this region occurred in February 2000 when Cleveland volcano (52.82° N, 167.95° W) erupted and sent an extensive plume of ash towards the north-northeast, in agreement with expectation based on the mean wind circulation—for animation of this event see: http://puff.images.alaska.edu/animations/Cleve_021901_76.gif. Some ash also moved in a south–southeast direction and intersected air traffic off the west coast of the USA. Four aviation encounters were reported in the vicinity of the volcano, and one encounter was reported off California at FL-300 with a B-747 (Simpson et al. 2002).

Aviation traffic is increasing and is expected to grow at a rate of between 2.2% to 4.7% per year for the period 1990–2050 (ESCAP 2005). There are significant regional differences in the current growth rate of commercial aviation traffic and also in the projected rates. Largest increases are expected in the Middle East and Asia Pacific regions, with many more commercial and freight traffic crossing the Pacific Rim. During 2004–2007 commercial air traffic grew at 8.6% for the Asia/Pacific region, compared to 6.8% for the world. The Middle East region grew at an annual average rate of 10.9%. Air freight traffic is also growing. For the period 2002–2015 air freight traffic is expected to grow at an annual average rate of 6.4% for the Asia Pacific, 6.6% for the Middle East and 5.5% globally (ESCAP 2005). The Asia Pacific region is also a region with many volcanoes—approximately 450, and about 50% of the world's active volcanoes lie along the Pacific Rim—the so-called "Ring of Fire". Coupled with the trend from using 4-engined jet aircraft to using twin-engined aircraft, there is a significant increase in vulnerability of the world's air traffic fleet to loss of aircraft due to encounters with a volcanic ash cloud.

Figure 7 shows an estimate of the global air traffic density based on the 2002 NOx emissions taken from the AERO2k emissions inventory (Eyres et al. 2004) for the month of October and for flight levels of FL 350 (pressure altitude of 33,000 ft) to FL 390 (39,000 ft). NOx emissions are used here as a proxy for air traffic density and are a good indicator of the global spatial pattern of air traffic. Also shown on this Figure are all

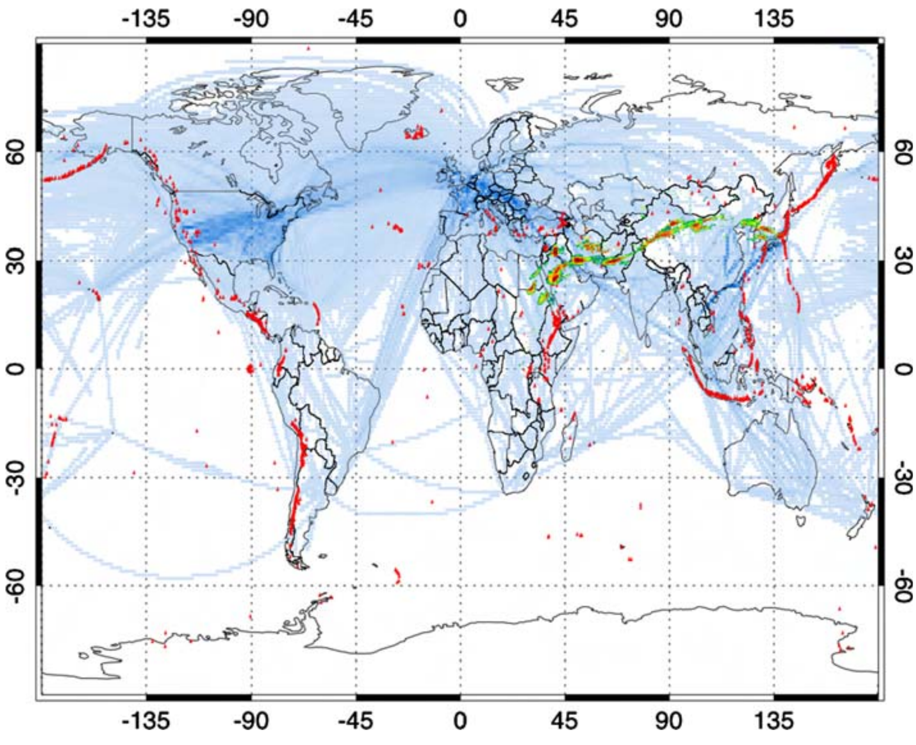

Fig. 7 Global density of air traffic as measured by monthly averaged NOx emissions for FL 350 to FL 390 (pressure altitudes of 33,000 ft up to 39,000 ft) taken from the AERO2k emissions inventory of Eyers et al. (2004). Emissions are shown for October 2002. The colour code is linearly scaled with greatest emissions represented as deepest blue. The red triangles indicate the positions of Holocene and Historically listed volcanoes taken from the Smithsonian database (Simkin and Siebert 1994). There are over 1,200 volcanoes indicated on the plot. The OMI SO_2 column observations from the eruption of Jebel at Tair during 1–10 October 2007 are also shown on this plot. These data are scaled to show the relative column amounts each day as observed by OMI, with red representing the highest values and green the lowest

Holocene and historically known volcanoes (Simkin and Seibert 1994). The greatest traffic densities are seen over Europe and North America, with noticeable air traffic trajectories across the north Atlantic (the NATs) and from Japan to south-east Asian population centres. To illustrate the vulnerability of air traffic to encounters with volcanic clouds, the OMI SO_2 cloud observations from the eruption of Jebel at Tair during 1–10 October, 2007 are overlaid onto the Figure. Eckhardt et al. (2008) estimate that the cloud travelled mostly just above the tropopause at altitudes between 14 and 16 km. As most commercial aircraft cruise at around 13 km (39,000 ft) this may not have been a problem for currently operating air traffic, however should fleets of HSCT aircraft operate in the future, dispersed volcanic debris, far from its source will become an increasing risk to these aircraft. Later modelled trajectories suggest that the cloud may have re-entered the troposphere and re-curved south and westwards towards India, where OMI also observed the cloud, albeit at much lower concentrations.

With increased air traffic over the Asia/Pacific region and with many active volcanoes located there, it is concluded that this region will become increasingly vulnerable to aviation/volcanic cloud encounters. The potential for an encounter is illustrated using the air traffic density forecast for 2025 and an eruption from a remote volcano located in the Northern Mariana Islands. During 2003 until the present, Anatahan volcano in the Northern Mariana Islands (16.35° N, 145.67° E) has been emitting ash clouds into the atmosphere at regular intervals. This volcano lies under an air route from Guam and Saipan to Japan and ash clouds from the volcano frequently intercept the major air routes from south-east Australia, and the Philippines to Japan and Korea. Figure 8 shows the coincidence of forecast April 2025 air traffic density (FL 350 to FL 390) with volcanoes and an AIRS SO_2 cloud from Anatahan for April 2005. This cloud covered an area of more than 1.3 million km^2 over 3 days in April, reached an altitude of at least 15 km ($\sim$48,000 ft) and air traffic was diverted on several occasions. The ash and gas cloud continued to spread westwards, eventually intercepting Philippine air space and continued on towards the South China Sea. At most times of the year, eruptions in this region are likely to send ash westwards and into busy air corridors involving south-east Asia, Japan, Korea and Australia.

6 Conclusions

Satellite instruments are able to identify and track hazardous ash and SO_2 clouds in the atmosphere for hours to several weeks. Ash has a considerably shorter lifetime ($\sim$hours) in the atmosphere than SO_2 ($\sim$days to weeks) and is more difficult to identify and quantify. Ash is much more hazardous to jet aircraft than SO_2 and has been responsible for several complete engine shut-downs and significant air-frame damage. Under favourable circumstances it appears that by tracking SO_2 clouds from satellite, the movement of the more hazardous ash clouds may be inferred, but care must be taken as there are documented cases (Schneider et al. 1999; Prata and Kerkmann 2007) where ash and SO_2 separate and travel in different directions and at different heights in the atmosphere. Operationally there are no reliable ash cloud height estimates available from satellites. The CALIPSO lidar can provide excellent height estimates for aerosols (H_2SO_4 aerosol in the case of volcanic clouds), but the poor horizontal spatial coverage and poor temporal coverage make the instrument inadequate for operational use. The recent study by Eckhardt et al. (2008) has shown that by using satellite estimates of volcanic cloud trajectories with Lagrangian dispersion models, the injection height profile of the volcanic eruption may be estimated.

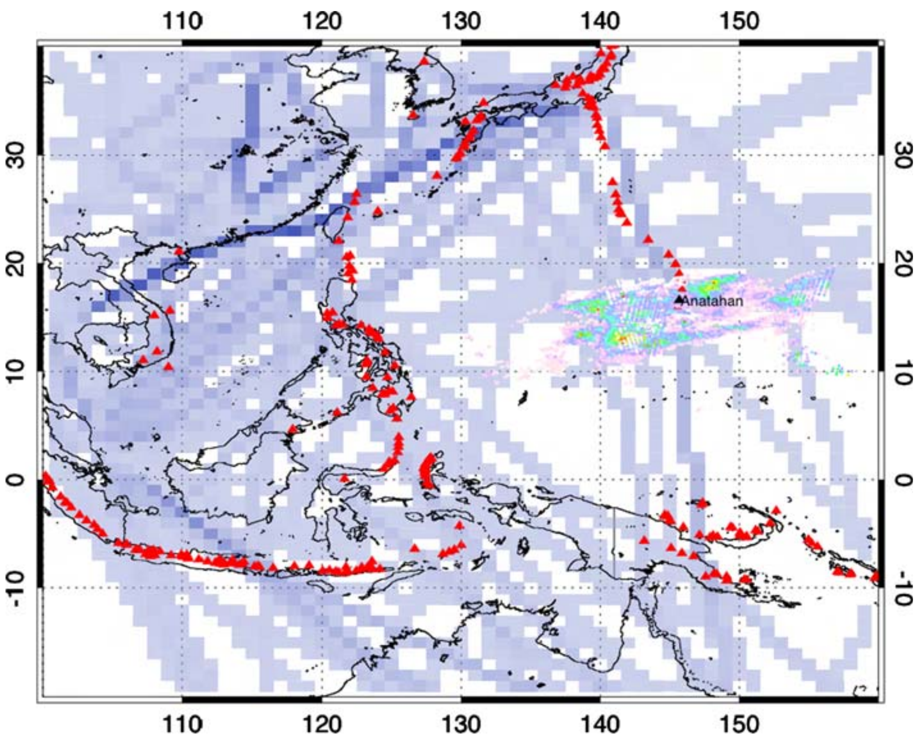

Fig. 8 Asia Pacific regional air traffic density from monthly averaged forecast NOx emissions for FL 350 to FL 390 (pressure altitudes of 33,000 ft up to 39,000 ft) taken from the AERO2k emissions inventory of Eyres et al. (2004). Forecast emissions are shown for April 2025. The colour code is linearly scaled with greatest emissions represented as deepest blue. The red triangles indicate the positions of Holocene and Historically listed volcanoes taken from the Smithsonian database (Simkin and Siebert 1994). There are over 450 volcanoes indicated on the plot. The AIRS SO_2 column observations from the eruption of Anatahan during 6–8 April 2005 are also shown on this plot. These data are scaled to show the relative column amounts each day as observed by AIRS, with red representing the highest values and lilac, the lowest

This much more objective estimate of the cloud height can then be used to forecast the cloud movement with greater confidence and accuracy. For some regions, where 15-min infrared data are available from geosynchronous satellites, it will be possible to reliably transmit accurate 3D trajectories of hazardous volcanic clouds for use by the aviation industry. By supplying height and horizontal spatial information on the location and movement of volcanic clouds, the aviation industry will be able to re-route air traffic as necessary and at the same time minimize the extra fuel used. Satellite data can also be used to identify volcanic clouds that are predominantly composed of SO_2 and/or volcanic ash. This information may be used by the aviation industry to determine the appropriate post-maintenance procedures required in the event of an encounter with a volcanic cloud. As ash is known to cause engine damage and clogging of pitot static tubes and SO_2 is not implicated in this kind of damage, there may be an economic advantage in utilizing this information.

It has been noted that commercial and freight air traffic is growing globally and regionally, with the Asia Pacific region experiencing one of the highest annual growth rates. The region also contains many volcanoes and is thus vulnerable to air traffic volcanic cloud encounters. The introduction of fleets of HSCT travelling at speeds of up to mach 2.5 and cruising at altitudes as high as 20 km will increase the aviation/volcanic cloud encounter risk. The much higher aircraft speeds will also demand much shorter warning times, suggesting a need for either a constellation of polar-orbiting instruments or a network (5–6) of geosynchronous rapid scan instruments. Vulnerability maps can be developed based on proxies for air traffic densities, which provide a good indication of the air traffic spatial habit. Atmospheric dispersion models are now capable of providing reliable forecasts of volcanic cloud movement for several days from the onset of eruption, provided good injection height information is available. The air traffic density maps, dispersion model runs, volcano locations and wind analyses provide the ingredients to develop scenarios for aviation/volcanic cloud encounters. These scenario generators can be used for examining risks and vulnerabilities and for examining potential problems should HSCT aircraft become operational.

Appendix

Table 4 List of acronyms

ASTER	Advanced Spaceborne Thermal Emission and Reflection Radiometer
AIRS	Atmospheric InfraRed Spectrometer
ATSR	Along-Track Scanning Radiometer
AVHRR	Advanced Very High Resolution Radiometer
CALIPSO	Cloud-Aerosol Lidar and Infrared Pathfinder Satellite Observations
GOES	Geosynchronous Orbiting Environmental Satellite
GOME	Global Ozone Monitoring Experiment
HIRS	High resolution InfraRed Sounder
HYSPLIT	HYbrid Single-Particle Lagrangian Integrated Trajectory
IASI	Infrared Atmospheric Sounding Interferometer
IR	InfraRed
MetOP	Operational meteorological satellite
MLS	Microwave Limb Sounder
MODIS	Moderate Resolution Imaging Spectroradiometer
MSG	Meteosat Second Generation
MUT	Mid- and Upper-Troposphere
NOAA	National Oceanographic and Atmospheric Administration
OMI	Ozone Monitoring Instrument
PUFF	Volcanic Ash Tracking Model
SCIAMACHY	SCanning Imaging Absorption SpectroMeter for Atmospheric Cartography
SEVIRI	Spinning Enhanced Visible and InfraRed Imager
TIROS	Television and Infrared Orbiting Satellite
TOMS	Total Ozone Mapping Spectrometer
UV	Ultra-Violet
VISSR	Visible and Infrared Spin Stabilized Radiometer

References

Barton IJ, Prata AJ, Watterson IG, Young SA (1992) Identification of the Mount Hudson volcanic cloud over SE Australia. Geophys Res Lett 19:1211–1214

Bernard A, Rose WI (1984) The injection of sulfuric acid aerosols in the stratosphere by the El Chichon volcano and its related hazards to the international air traffic. Nat Hazards 3(1):59–67. doi:10.1007/BF00144974

Bluth GJS, Schnetzler CC, Krueger AJ, Walter LS (1993) The contribution of explosive volcanism to global atmospheric sulphur dioxide concentrations. Nature 366:327–329

Carn SA, Krueger AJ, Krotkov NA, Gray MA (2004) Fire at Iraqi sulfur plant emits SO_2 clouds detected by Earth Probe TOMS. Geophys Res Lett 31:L19105. doi:10.1029/2004GL020719

Carn SA, Krotkov NA, Yang K, Hoff RM, Prata AJ, Krueger AJ, Loughlin SC, Levelt PF (2007) Extended observations of volcanic SO_2 and sulphate aerosol in the stratosphere. Atmos Chem Phys Discuss 7:2857–2871

Carn SA, Prata AJ, Karlsdottir S (2008) Circumpolar transport of a volcanic cloud from Hekla (Iceland). J Geophys Res 113. doi:10.1029/2008JD009878

Casadevall TJ (1994) The 1989/1990 eruption of Redoubt Volcano Alaska: impacts on aircraft operations. J Volcanol Geotherm Res 62(30):301–316

Casadevall TJ, Delos Reyes PJ, Schneider DJ (1996) The 1991 Pinatubo eruptions and their effects on aircraft operations. In: Newhall CG, Punongbayan RS (eds) Fire and mud: eruptions and lahars of Mount Pinatubo, Philippines. Philippines Institute of Volcanology and Seismology, Quezon City, University of Washington Press, Seattle, pp 625–636

Chahine MT, Pagano TS, Aumann HH, Atlas R, Barnet C, Blaisdell J, Chen L, Divakarla M, Fetzer EJ, Goldberg M, Gautier C, Granger S, Hannon S, Irion FW, Kakar R, Kalnay E, Lambrigtsen BH, Lee S-Y, LeMarshall J, McMillan WW, McMillin L, Olsen ET, Revercomb H, Rosenkranz P, Smith WL, Staelin D, Strow LL, Susskind J, Tobin D, Wolf W, Zhou L (2006) AIRS: improving weather forecasting and providing new data on greenhouse gases. Bull Am Meteorol Soc 87:910–926. doi:10.1175/BAMS-87-7-911

Clerbaux C, Hadji-Lazaro J, Turquety S, George M, Coheur P-F, Hurtmans D, Wespes C, Herbin H, Blumstein D, Tournier B, Phulpin T (2007) The IASI/MetOp I mission: first observations and highlights of its potential contribution to GMES. COSPAR Inf Bull 2007:19–24

Constantine EK, Bluth GJS, Rose WI (2000) TOMS and AVHRR sensors applied to drifting volcanic clouds from the august 1991 eruptions of Cerro Hudson. In: Mouginis-Mark P, Crisp J, Fink J (eds) AGU Monograph 116—Remote Sensing of Active Volcanism, pp 45–64

Eckhardt S, Prata AJ, Seibert P, Steibel K, Stohl A (2008) Estimation of the vertical profile of sulfur dioxide injection into the atmosphere by a volcanic eruption using satellite column measurements and inverse transport modeling. Atmos Chem Phys Discuss 8:3761–3805

Eisinger M, Burrows JP (1998) Tropospheric sulfur dioxide observed by the ERS-2 GOME instrument. Geophys Res Lett 25(22):4177–4180

Ellrod GP, Connell BH, Hillger DW (2003) Improved detection of airborne volcanic ash using multispectral infrared satellite data. J Geophys Res 108(D12):4356. doi:10.1029/2002JD002802

ESCAP (2005) Review of developments in transport in Asia and the Pacific 2005, United Nations Publ., No. E.06.II.F.9, ST/ESCAP/2392, 172 pp

Eyers CJ, Norman P, Middel J, Michot S, Atkinson K, Christou RA (2004) AERO2k global aviation emissions inventories for 2002 and 2025. European Commission Contract, No. G4RD-CT-2000-00382, QINETIQ/04/0113, 144 pp

Fleming EL, Chandra S, Shoeberl MR, Barnett JJ (1988) Monthly mean global climatology of temperature, wind, geopotential height and pressure for 0–120 km. National Aeronautics and Space Administration, Technical Memorandum 100697, Washington, DC

Guffanti M, Albersheim S (2008) The United States national volcanic ash operations plan for aviation. Nat Hazards Special Issue: Aviation hazards from volcanoes. doi:10.1007/s11069-008-9247-1

Hanstrum BN, Watson AS (1983) A case study of two eruptions of Mount Galunggung and an investigation of volcanic eruption cloud characteristics using remote sensing techniques. Aust Meteorol Mag 31:131–177

Hillger DW, Clark JD (2002a) Principal component image analysis of MODIS for volcanic ash. Part I: most important bands and implications for future GOES imagers. J Appl Meteorol 41:985–1001

Hillger DW, Clark JD (2002b) Principal component image analysis of MODIS for volcanic ash. Part II: simulation of current GOES and GOES-M imagers. J Appl Meteorol 41:1003–1010

Holasek RE, Rose WI (1991) Anatomy of 1986 Augustine volcano eruptions as recorded by multispectral images processing of digital AVHRR weather satellite data. Bull Volcanol 53:42–435

Holasek RE, Woods AW, Self S (1996) Experiments on gas-ash separation processes in volcanic umbrella clouds. J Volcanol Geotherm Res 70:169–181
Krotkov NA, Carn SA, Krueger AJ, Bhartia PK, Yang K (2006) Band residual difference algorithm for retrieval of SO_2 from the Aura Ozone Monitoring Instrument (OMI). IEEE Trans Geosci Remote Sens 44(5):1259–1266
Krueger AJ (1983) Sighting of El Chichon sulfur dioxide clouds with the nimbus 7 total ozone mapping spectrometer. Science 220:1377–1379
Krueger AJ, Walter LS, Bhartia PK, Schnetzler CC, Krotkov NA, Sprod I, Bluth GJS (1995) Volcanic sulfur dioxide measurements from the total ozone mapping spectrometer instruments. J Geophys Res 100(D7):14057–14076
Krueger AJ, Schaefer SJ, Krotkov N, Bluth GJS, Baker S (2000) Ultraviolet remote sensing of volcanic emissions. In: Mouginis-Marks PJ, Crisp JA, Fink JH (eds) Remote sensing of active volcanism. Geophys Monogr Ser 116:2543, AGU, Washington, DC
Malingreau J, Kaswanda P (1986) Monitoring volcanic eruptions in Indonesia using weather satellite data: the Colo eruption of July 28, 1983. J Volcanol Geotherm Res 27(1–2):179–194
Matson M (1984) The 1982 El Chichon volcano eruptions—a satellite perspective. J Volcanol Geotherm Res 23:1–10
Miller TP, Casadevall TJ (1999) Volcanic ash hazards to aviation. In: Sigurdsson H, Houghton B, McNutt SR, Ryman H, Stix J (eds) Encyclopedia of volcanoes. Academic Press, San Diego, pp 915–930
Mosher FR (2000) Four channel volcanic ash detection algorithm, Preprint Volume. 10th Conference on Satellite Meteorology and Oceanography, Long Beach, California, 9–14 January, 2000, pp 457–460
Pavolonis MJ, Feltz WF, Heidinger AK, Gallina GM (2006) A daytime complement to the reverse absorption technique for improved automated detection of volcanic ash. J Atmos Oceanic Technol 23:1422–1444
Pergola N, Tramutoli V, Marchese F, Scaffidi I, Lacav T (2004) Improving volcanic ash cloud detection by a robust satellite technique. Remote Sens Environ 90:1–22
Pieri D, Ma C, Simpson JJ, Hufford G, Grindle T, Grove C (2002) Analyses of in-situ airborne ash from the February 2000 eruption of Hekla volcano, Iceland. Geophys Res Lett 29:16. doi:10.1029/2001GL013688
Prata AJ (1989a) Observations of volcanic ash clouds using AVHRR-2 radiances. Int J Remote Sens 10(4–5):751–761
Prata AJ (1989b) Radiative transfer calculations for volcanic ash clouds. Geophys Res Lett 16(11):1293–1296
Prata AJ, Grant IF (2001) Retrieval of microphysical and morphological properties of volcanic ash plumes from satellite data: application to Mt. Ruapehu, New Zealand. Q J R Meteorol Soc 127(576B):2153–2179
Prata AJ, Kerkmann J (2007) Simultaneous retrieval of volcanic ash and SO_2 using MSG-SEVIRI measurements. Geophys Res Lett 34:L05813. doi:10.1029/2006GL028691
Prata AJ, Bluth GJS, Rose WI, Schneider DJ, Tupper AC (2001) Comments on Failures in detecting volcanic ash from a satellite-based technique. Remote Sens Environ 78:341–346
Prata AJ, Rose WI, Self S, O'Brien DM (2003) Global, long-term sulphur dioxide measurements from TOVS data: a new tool for studying explosive volcanism and climate. Volcanism and the Earth's atmosphere, geophysics monograph 139 AGU, pp 75–92
Prata AJ, Carn SA, Stohl A, Kerkmann J (2007) Long range transport and fate of a stratospheric volcanic cloud from Soufriere ills volcano, Montserrat. Atmos Chem Phys 7:5093–5103
Richardson AJ (1984) El Chichon volcanic ash effects on atmospheric haze measured by NOAA-7 AVHRR data. Remote Sens Environ 16:157–164
Richter A, Wittrock F, Burrows JP (2006) SO_2 measurements with SCIAMACHY. In: Proceedings of the first conference on atmospheric science, Frascati, Italy, 8–12 May 2006. ESA publication SP-628
Rose WI, Delene DJ, Schneider DJ, Bluth GJS, Kruger AJ, Sprod I, McKee C, Davies HL, Ernst GJ (1995) Ice in the 1994 Rabaul eruption: implications for volcanic hazard and atmospheric effects. Nature 375:477–479
Sawada Y (1987) Study on analysis of volcanic eruptions based on eruption cloud image data obtained by the Geostationary Meteorological Satellite (GMS). Technical reports of the Meteorological Research Institute, vol 22, 335 pp
Sawada Y (1996) Detection of explosive eruptions and regional tracking of volcanic ash clouds with geostationary meteorological satellites (GMS). In: Scarpa R, Tilling RI (eds) Monitoring and mitigation of volcano hazards. Springer-Verlag, Berlin, Heidelberg, pp 299–314
Schneider DJ, Rose WI, Kelley L (1995) Tracking of 1992 eruption clouds from Crater Peak of Mount Spurr volcano, Alaska, using AVHRR. US Geol Surv Bull 2139:27–36

Schneider DJ, Rose WI, Coke LR, Bluth GJS (1999) Early evolution of a stratospheric volcanic eruption cloud as observed with TOMS and AVHRR. J Geophys Res 104(D4):4037–4050

Simkin T, Seibert L (1994) Volcanoes of the world, 2nd edn. Geoscience Press, Tucson

Simpson JJ, Hufford G, Pieri D, Berg J (2000) Failures in detecting volcanic ash from a satellite-based technique. Remote Sens Environ 72:191–217

Simpson JJ, Hufford G, Pieri D, Servranckx R, Berg J (2002) The february 2001 eruption of Mount Cleveland, Alaska: case study of an aviation hazard. Weather Forecast 17:691–704

Thomas W, Erbertseder T, Ruppert T, Van Roozendael M, Verdebout J, Balis D, Meleti C, Zerefos C (2004) On the retrieval of volcanic sulfur dioxide emissions from GOME backscatter measurements. J Atmos Chem 50:295–320. doi:10.1007/s10874-005-5079-5

Torres O, Bhartia PK, Herman JR, Ahmad Z, Gleason J (1998) Derivation of aerosol properties from satellite measurements of backscattered ultraviolet radiation: theoretical basis. J Geophys Res 103(D14):17099–17110

Tupper A, Carn SA, Davey J, Kamada Y, Potts RJ, Prata AJ, Tokuno M (2004) An evaluation of volcanic cloud detection techniques during recent significant eruptions in the western ring of fire. Remote Sens Environ 91:27–46

Urai M (2004) Sulfur dioxide flux estimation from volcanoes using advanced spaceborne thermal emission and reflection radiometer—a case study of Miyakejima volcano, Japan. J Volcanol Geotherm Res 134(1–2):1–13

Van Geffen J, Van Roozendael M, Di Nicolantonio W, Tampellini L, Valks P, Erbetseder T, Van der AR (2007) Monitoring of volcanic activity from satellite as part of GSE PROMOTE. Proceedings of the first conference on atmospheric science, Frascati, Italy, 8–12 May 2006. ESA publication SP-628

Watkin SC (2003) The application of AVHRR data for the detection of volcanic ash in a volcanic ash advisory centre. Meteorol Appl 10:301–311

Wei C-F, Larson SM, Pattena KO, Wuebbles DJ (2001) Modeling of ozone reactions on aircraft-related soot in the upper troposphere and lower stratosphere. Atmos Environ 35:6167–6180

Wen S, Rose WI (1994) Retrieval of sizes and total masses of particles in volcanic clouds using AVHRR bands 4 and 5. J Geophys Res 99(D3):5421–5431

Witham CS, Hort MC, Potts R, Servranckx R, Husson P, Bonnardot F (2007) Comparison of VAAC atmospheric dispersion models using the 1 November 2004 Grimsvtn eruption. Meteorol Appl 14:27–38

Yu T, Rose WI, Prata AJ (2002) Atmospheric correction for satellite-based volcanic ash mapping and retrievals using split window IR data from GOES and AVHRR. J Geophys Res 107(D16):4311. doi:10.1029/2001JD000706